VOL. 12, NO. 21, NOVEMBER 2017 ISSN 1819-6608
ARPN Journal of Engineering and Applied Sciences

www.arpnjournals.com

THE ROLE OF TIC ON THE HARDNESS AND WEAR RESISTANCE OFAA 7075 USING GTA

R. Prashanth, A. Shanmugasundaram, J. Abhinavaram and S. Jagadeesh
Department of Mechanical Engineering, Amrita University, Coimbatore, India
E-Mail: a_shanmugasundaram@cb.amrita.edu

ABSTRACT

The main objective of this study is to improve the hardness and wear resistance of AA 7075 by reinforcing Titanium Carbide (TiC) particles onto the aluminium alloy surface using Gas Tungsten Arc (GTA) as a heat source. Based on the number of trails, optimum GTA heat source parameters are finalized with reference to the proper fusion of base metal. After TiC is deposited onto the surface, three step post-weld heat treatment (PWHT) was employed to improve the hardness and wear resistance. The material was solution treated followed by water quenching and artificially aged. The Dry sliding wear tests were conducted using a pin on disc wear testing equipment and the wear rates were calculated by using weight loss method. An inverse relationship was found between wear rate and hardness. The increase in the microhardness was found to be 33 %. The wear rate increased with increase in the load but reduced with respect to increasing sliding velocity. The variation of COF with hardness was found to be almost constant. A detailed material characterization of as received AA 7075, after TiC reinforcement and after heat treating AA 7075 substrate was done using Scanning Electron Microscope (SEM), line - Energy dispersive X - ray spectrometry (Line-EDX) and X-ray diffraction (XRD) techniques.

Keywords: titanium carbide, GTA, AA 7075, artificial aging, surface modification, dry sliding wear test, hardness.

INTRODUCTION

Aluminium alloys are the second most widely used in the market next to steel. They are available in the various cast and wrought forms. The 7xxx series of aluminium alloys are obtained as wrought products. These alloys contain zinc as the primary alloying element along with copper and magnesium. Among the 7xxx series of aluminium alloys, 7075 has been a favorite choice in automobile, aerospace and marine industries due to its low density, high thermal conductivity and high strength [1]. However, its applications are limited due to its poor hardness and tribological behavior.

The hardness and wear properties can be improved by the application of heat, changing the elemental composition, cryogenic treatment, etc., in the bulk or at the surface. A lot of investigations were already done on aluminium metal matrix composites. Work has already been carried out on altering the elemental composition of bulk materials of Zn-Al-Si alloys [2] and Al-Zn-Cu alloys [3] by using stir casting technique. Wear rates of Al-6Zn-4Mg alloys were tested at different conditions [4]. Effect of shallow cryogenic treatment on hardness and microstructure using GTAW process was also studied [5].

Effect of reinforcements of ceramic particles like SiC, Al_2O_3, TiC on the substrate of the aluminium alloy was already tested [6-8]. It was observed that wear behavior is dependent on metal matrix hardness of AA 6061-Al_2O_3 composites [9]. In-situ reinforcement of TiB_2 and its effect on AA 7075 wear resistance is also studied [10]. Although these bulk modification techniques were successful in improving surface properties, on the downside, there is a possibility for reduction in toughness and occurrence of non-homogeneous reinforcements on the bulk substrate. Moreover, the tribological behavior of an alloy is a surface phenomenon. Hence, the hardness and wear resistance could be improved by surface modification rather than by bulk modification.

Surface modifications can be done by application of heat using GTA, Friction Stir processing, laser cladding, thermochemical and electrochemical techniques such as Chemical Vapour deposition (CVD) and electroplating. The effect of friction stir process tool parameters on AA 7075-T6 joints was studied [11]. 6061 and 7005 aluminium alloys were reinforced with Al_2O_3 using friction stir processing and its effect on microstructure and mechanical properties were observed [12]. Selection of sizes and design of the pins used as consumable in the friction stir processes are some of the limitations. There is a restriction in the position of the sample during the process due to the orientation of the machine and the tool. At the end of the work, a keyhole is formed. In addition, the speed of the process is usually slower than that of fusion welding [13]. AISI 1045 steel surfaces were alloyed with Titanium Carbide using TIG as a heat source and its effect on hardness and wear properties were investigated by X.H. Wang *etal* [14]. Using GTA, the heat input to the materials can be greatly controlled by varying the various heat source parameters like heat source current, standoff distance, and specimen speed. In addition to the control of heat input to the material, the shielding gas Argon employed during the process helps in avoiding the oxidation effect and clean fusion surface can be obtained. Thereby, GTA proves to be the better alternative for surface modification.

Titanium carbide (TiC) is an extremely hard refractory ceramic material with high strength, rigidity and outstanding wear resistance. It has the appearance of black powder with the face-centered cubic crystal structure. It occurs in nature as a form of the very rare mineral khamrabaevite - (Ti,V,Fe)C [15]. The high resistance to solid state welding and lower coefficient of friction along with good stability at high temperature has made it a major

industrial material as secondary carbide in cemented tungsten carbide cutting and grinding tools. Due to good mechanical and abrasive wear characteristics, it is also used as a coating for these tools.

So far no investigation was done on surface modification of AA 7075 alloy using GTAW process. In this study, an attempt has been made to improve the hardness and wear characteristics of AA 7075 by reinforcing TiC on the surface using GTA as a heat source. Further, heat treatment of surface refined AA7075 is carried out and its effect on hardness and wear resistance are reported.

EXPERIMENTAL PROCEDURE

The procured AA7075 profile was the in the form of 300mm × 300mm × 12mm. The samples were prepared with dimensions 100mm × 25mm × 12mm from the purchased plate.

Lincoln Electric V205T GTAW equipment is used for applying heat over the surface of the AA 7075. A PLC based stepper motor driven manipulator is used to control the speed of the specimen, which is kept over the worktable. The position of the torch is held stationary in the vertically down position. Inert gas Argon is used as a shielding gas at 7 lpm flow rate. Thoriated tungsten electrode of diameter 2.4 mm is used during welding to have the better arc stability. Direct Current Electrode Negative (DCEN) mode is used. A schematic representation of the experimental setup is shown inFigure-1.

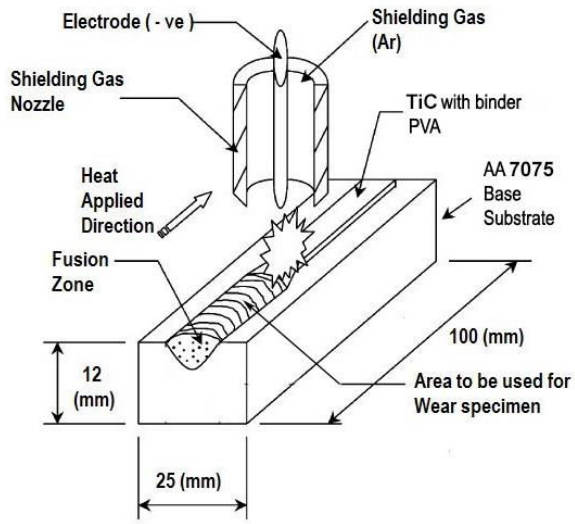

Figure-1. Schematic diagram of GTA setup.

Trial runs performed on the base metal by varying current (100 A to 200 A), work speed (1 to 10 mm/s.) and the electrode to work distance (1 to 5 mm). Thoriated tungsten electrode frequently grounded to maintain an angle of 60° at the tip. It was found that if the heat source current was below 150 A, the work speed was above 6 mm/s and the electrode to work distance was greater than 2mm then the lack of fusion was observed. If the current is above 150 A, work speed was below 2 mm/s and electrode to work distance were below 2 mm burn through were observed. The final heat source parameters reported in Table-1.

Table-1. Constant GTA parameters.

S. No.	GTA Process parameters	Unit	Value
1	Heat source current	A	150
2	Voltage	V	16
3	Distance between electrode and workpiece	mm	2
4	Work Speed	mm/s.	2, 4 & 6.
5	Electrode tip angle	Degree	60°

The commercially obtained TiC particles were sieved using the auto sieve-shaker. The different sieves used for the process of segregation are 38 µm, 76 µm, 106 µm, 150 µm, 220 µm and 300 µm. A major amount of TiC particles segregated in the 106 µm size and hence it has been used for the present investigation. In order to reinforce the TiC ceramic particle over the surface of AA 7075, it is necessary that the ceramic particles have to be bonded to the surface of the substrate. Otherwise, the particle will fly over to other areas due to the flow of inert gas during welding. Hydrolyzed Polyvinyl alcohol (PVA) was used as a binder. Titanium Carbide and polyvinyl alcohol is weighed equally and mixed thoroughly with heated water and stirred to become a paste so that the homogenized mixture of PVA and TiC is deposited over the surface of AA 7075. The specimens were kept in the furnace to remove the moisture. After it is dried in the furnace the specimens with bonded PVA cum Titanium carbide are ready for reinforcing onto the base metal. The TiC Particles were then reinforced onto the surface of the substrate using GTA as a heat source at the optimized process parameters.

After the TiC is reinforced onto the surface using GTA as a heat source, the substrate has to be subjected to post weld heat treatment process (PWHT) in order to improve their mechanical properties. The PWHT consists of three stages and is as follows:

a) Solution heat treatment at the temperature of 480° C for 2 hours as per the ASM standard.

b) Then, the solutionized specimens were quenched in water for about 10-15 minutes to get the supersaturated solid solution state.

c) After quenching, the specimens were artificially aged at the temperature of 120° C for 28 hours. The specimens were sliced into 9 pieces and tested for a differentaging period of 4, 8, 12, 16, 20, 22, 24, 26 and 28 hours.

The pin-on-disc wear test was conducted to investigate the dry sliding wear behavior of base metal, heat applied specimens and heat treated as well as surface refined substrate. Pin specimens of 8 mm diameter and 40 mm height were prepared from the above categories of substrates. The test was conducted at room temperature (30 °C) according to the ASTM G99-95a standard. The wear disc made of EN 31 material with the diameter of 165 mm, having the hardness of 60 HRC was used to slide against the pin surface. The wear testing parameters considered for dry sliding wear test are applied load (10, 20 and 30N) and sliding velocity (1, 1.5 and 2 m/s.) with a constant sliding distance of 1000m. On completion of each test, the specimen was removed, cleaned with acetone, dried and weighed to determine the weight loss due to wear, an electronic balance with an accuracy of 1mg was used to calculate the weight loss. The wear rates and COF of the samples were reported.

Microstructural analysis with Optical Microscope, SEM along with line EDAX and XRD were carried out to confirm the presence of TiC particle in AA 7075.

RESULTS AND DISCUSSIONS

The elements present in the base material confirmed by the Laser Spectroscopic analysis. Table-2 shows the chemical composition of the base material using Optical Emission Spectrometer (METAVISION - 1008 I). The microhardness of all the samples was measured using Mitutoyo Vickers microhardness testing equipment with 100 gfload for 15 seconds. Minimum of 10 points are used to get the average microhardness. The average microhardness of the base metal is 166 HV. The hardness and elemental compositions of the base material match with the AA 7075 under T6 temper condition in accordance with ASM standards.

Table-2. Elemental compositions of base material.

Element	Wt. %	Element	Wt. %
Zn	5.180	Mg	2.275
Cu	1.690	Fe	0.466
Si	0.060	Mn	0.056
Cr	0.204	Ti	0.052
Pb	0.059	Zr	0.013
Ca	0.002	Sr	0.002
Al.	Remaining		

AA 7075 in the T6 temper condition has a heterogeneous microstructure, consisting of an Al matrix, second phase particles and grain boundary regions. The aluminium alloy matrix contains a wide range of secondary phase particles that have been classified into three categories viz., precipitates, dispersoids and constituent particles. Precipitates are the smallest of these and are found to nucleate and grow during aging as a result of supersaturation of alloying elements after solutionization. The most notable precipitate is the η and ή phases of $MgZn_2$ and the associated solute-rich clusters known as GP zones. These precipitates are responsible for providing the high strength of the alloy. Alloying elements are added to 7xxx alloys mainly for precipitation hardening. Zinc and magnesium offer the highest potential for strengthening through age-hardening.

The various precipitates within the matrix of AA 7075, are Mg_2Al_3, Al_2Cu, $Al_{32}Zn_{49}$ and $MgZn_2$. The η and ή phases of $MgZn_2$are the major reason behind the AA7075 exhibiting high strength and hardness. They are identified as nano-sized precipitates along the grain boundaries [16,17].

The heat was applied to the specimens using heat source current as 150 A and 175 A by varying the specimen speed as 2, 4 and 6 mm/s. The heat inputs for the specimens were calculated with reference to the equation-1 [18]. The variation of heat input with specimen speed and the heat source current is shown in Figure-2.

$$q/_V = \frac{EI\eta}{V} \quad (1)$$

Where,
$q/_V$ Corresponds to heat input (J/mm),
E refers to the voltage (V),
I is the welding current (A),
V refers to the work specimen speed (mm/s.),
And η is the efficiency of GTA = 0.74 [19]

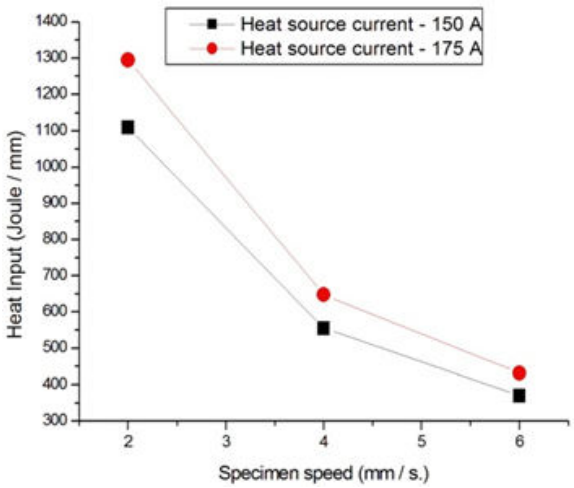

Figure-2. Profile of the Heat Input to the specimens with reference to the heat source current and specimen speed.

The heat input values for the heat source current of 150 A are 1110, 555 & 370 J/mm and for the heat source current of 175 A are 1295, 648 & 432 with respect to the work speed 2, 4 and 6 mm/s, respectively.

MICROSTRUCTURE ANALYSIS WITH LINE EDX OF BASE METAL

Figure-3 depicts the optical microscopy of the polished surface of the base metal AA7075. It is observed that there is the presence of dark patches and elongated

grains on the matrix of the alloy. The dark patches are secondary phase particles comprising Al_7Cu_2Fe, $(Al,Cu)_6(Fe,Cu)$, Al_3Fe and Al_2CuMg in the 10-20 µm range. They are the largest of secondary phase particles known as constituent particles. These particles are formed due to the process of solidification; breakage and alignment of such particles take place during forming and working with metal [20, 21, 22]. Researchers reveal that fine precipitates ($MgZn_2$) in the grains and coarse precipitates are present along the grain boundaries. The high hardness exhibited by AA 7075 is due to them. Apart from this, the high strength of T6 microstructure is mainly due to GP zones and ή precipitates, but the contribution of ή precipitates to the strength was reported to be higher [22].

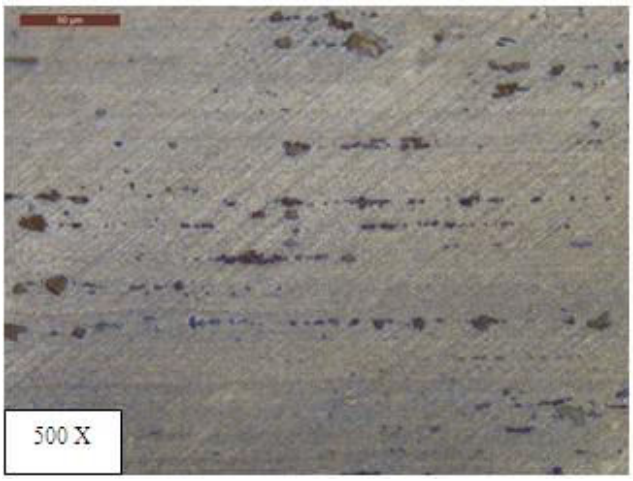

Figure-3. Microstructure of base metal AA 7075 at 500 X.

In order to identify the phases, which dominate these constituent particles, an EDX analysis was done on the as received AA 7075. During the line EDX analysis, a line was made to pass through the various types of constituent particles, which helps us to obtain clear information about the elements across the region over which the line was drawn.

The EDX line scan is shown inFigure-4. It reveals that the presence of Silicon, Iron, zinc, Magnesium, copper and iron in the alloy matrix.

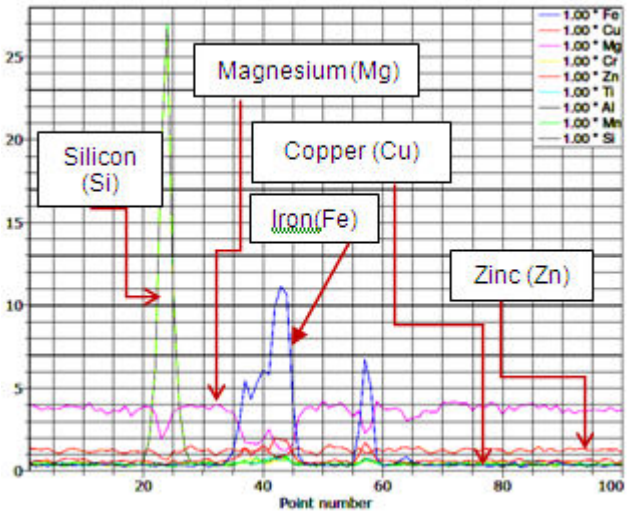

Figure-4(a). Line EDX scan of base metal AA 7075.

Based on the literature survey, it was found that the large constituent particles consist of Al_7Cu_2Fe, Al_2Cu (θ-phase) and Al_3Fe (β-phase), while smaller particles containing magnesium and silicon consist of Mg_2Si (β-phase). In addition to that, precipitation of Magnesium and zinc takes place along the grain boundaries as $MgZn_2$ (η-phase) [20, 21, 22].

HARDNESS ANALYSIS OF HEAT APPLIED SPECIMEN

The heat was applied at a constant standoff distance of 2 mm with the varying heat source current (150 A, 175 A) and specimen speed (2mm/s, 4mm/s and 6mm/s). Microhardness measurements were measured in the fusion zone, heat affected zone and base metal of heat applied specimens. The variation in microhardness of the heat applied samples with the sample speed of 2mm/s, 4 mm/s & 6 mm/s for welding current of 150A and 175 A are shown in Figures 5 (a) & 5 (b) respectively. Figure-8 depicts the consolidated hardness reduction of all the 6 trials.

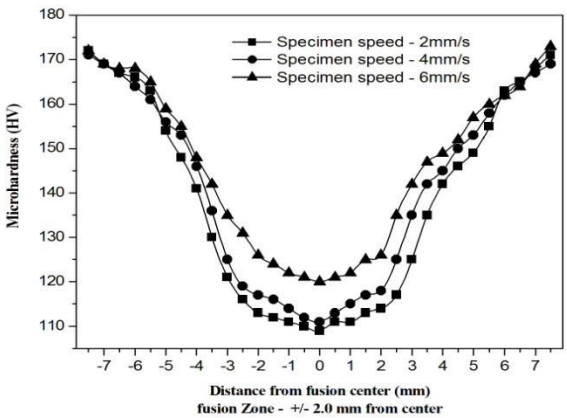

Figure-5(a). Microhardness (HV) of heat applied specimens with heat source current of 150 A.

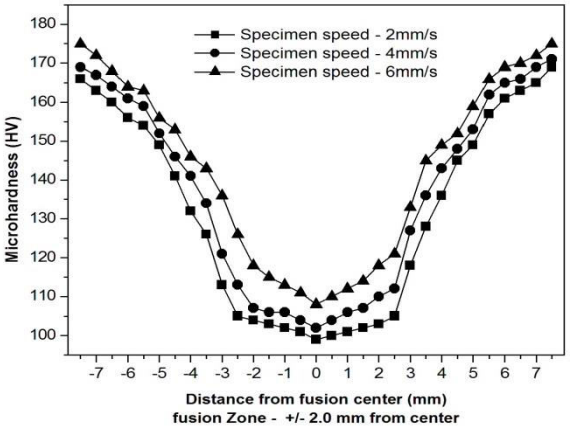

Figure-5(b). Microhardness (HV) of heat appliedspecimens with heat source current of 175 A.

When the heat source current is 150 A and the work speed is 2, 4 and 6 mm/s, then the hardness at the center of the fusion zone is found to be 113, 116 and 124 HV respectively. With the same range of work speed and with the heat source current of 175 A, the hardness at the center of the fusion zone is found to be 102, 107 and 115 HV. The hardness decreases maximum at the center of the fusion zone. In addition, it is found that the hardness is decreased when the speed is decreased. With reference to, the Figure 5 (a) and 5 (b) it can be inferred that there is a variation in hardness across the width of the base plate. The hardness at the edge of the plate is almost closer to the base metal hardness value because of the heat dissipation at the edges are more compared to the fusion zone and the effect of heat in turns of hardness reduction is not much in the edges. Whereas at the center of the fusion zone, the heat input was constant, but the heat dissipation was much lesser compared to the other places of the specimen. This causes the center of the fusion zone to have lower hardness when compared to other places of the specimen.
The difference in the solidification rate across different regions namely fusion zone, heat affected zone (HAZ) and the base metal is the reason behind the varying hardness measurements obtained. The heat dissipation is higher on the extreme left and right of the weld zone, farther away from the HAZ. Hence, the effect of heat is reduced. On the contrary, the heat dissipation was almost nil on the center of the fusion zone due to a constant supply of heat input. This justifies the fact of fusion zone having lower hardness compared to the extreme left and right side of the weld zone.

For the heat source current of 150 A, the percentage reduction in hardness on the fusion zone with reference to the base metal (166 HV) was 32.39 %, 30.81 % and 25.75 % for the specimen speed of 2 mm/s, 4 mm/s and 6 mm/s respectively. Similarly, for the heat source current of 175 A, the percentage reduction in hardness on the fusion zone was 38.76 %, 36.09 % and 31.08 % as compared to base metal.

From the above results, it is observed that after application of heat maximum reduction in hardness occur in the fusion zone. The aluminium grain size, dislocation density along with dissolution, nucleation, growth and distribution of precipitates needs to be taken into account to understand this behavior of reduction in hardness. Due to a large amount of heat applied during GTA process, dissolution of ή precipitates and coarsening of the grains in the aluminium matrix occur, thereby resulting in reduced hardness. But the presence of some fine equiaxed grains and the resolution of the dissolved precipitates partially remedy the loss of hardness

On the basis of 6 trials conducted, the maximum reduction in hardness of the fusion zone was observed in the case of 175 A & 2 mm/s. The hardness was measured to be 102 HV and the reduction from the base metal hardness of 166 HV is 38.76 %. (64 HV).Whereas, the minimum reduction in hardness was observed in the case of 150 A & 6 mm/s. The average hardness is 124 HV and the reduction in hardness with respect to the base metal is only 25.75 % (42 HV). This was in accordance to heat input calculations done earlier as a higher reduction in hardness values are observed as the heat input values are increased. Thus, the remaining part of the study will be carried on at 150 A & 6 mm/s, as it has the least reduction in hardness.

MICROSTRUCTURE ANALYSIS OF HEAT APPLIED SAMPLES

The optical micrographs of the fusion zone of samples processed with 150 A & 6 mm/s and with 175 A & 2 mm/s are shown in figure 6 (a) and 6 (b) correspondingly. Both the specimens were observed at 500X. The specimen with a heat source current of 150 A & work speed of 6 mm/s experiences lower heat input and hence the heat penetration and width of the fusion zone is less. The heat dissipation to the base metal is higher in this case. Hence, the solidification will happen at a faster rate, which leads to the formation of finer grains. On the contrary, the specimen with a heat source current of 175 A & work speed of 2 mm/s has a higher heat input and a slower rate of solidification as the heat dissipation to the base metal is much lesser resulting in the formation of coarser grains in the case of this sample.

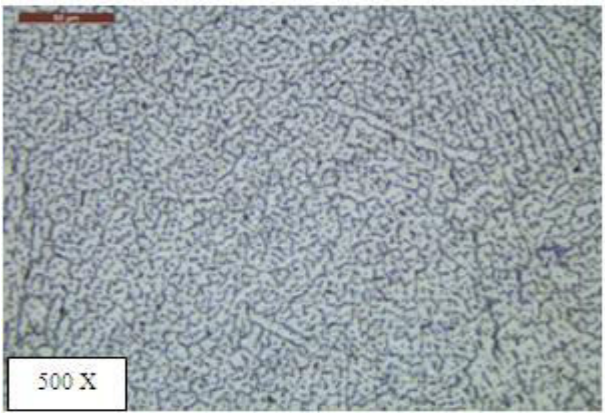

Figure-6(a). Fusion zone micrographs of heat applied sample of 150 A & 6 mm/s (500 X).

The finer grains in the 150 A & 6 mm/s specimen is the reason for its higher hardness at the weld zone when compared to the other specimen. This micrographic study further explains the higher hardness of the latter. This is in line with the Hall -Petch equation which states that hardness increases as grain size decreases [23]. Also, the small particles of the intermetallic compounds formed as shown in Figure-6 (a), are also a benefit to hardness improvement according to Orowan hardening mechanism [24].

Hence, the future study will be carried on setting the welding current at 150 A and the welding speed at 6 mm/s, as our ultimate aim is to increase the hardness of AA 7075 upon reinforcing ceramic particles.

FE - SEM was carried out on the heat-applied sample and is shown inFigure-7. The figure indicates the Fusion zone, heat affected zone and base metal of the heat-applied specimen observed at 2,000X. The constituent particles of the fusion zone are much coarser than those of the heat affected zone. This is because of the higher temperature and slower solidification rate in the fusion zone when compared to the heat affected zone. Whereas the constituent particles of the base metal are finer than the particles of the heat affected zone. This is because of the higher temperature and slower solidification rate in the heat-affected zone when compared to base metal.

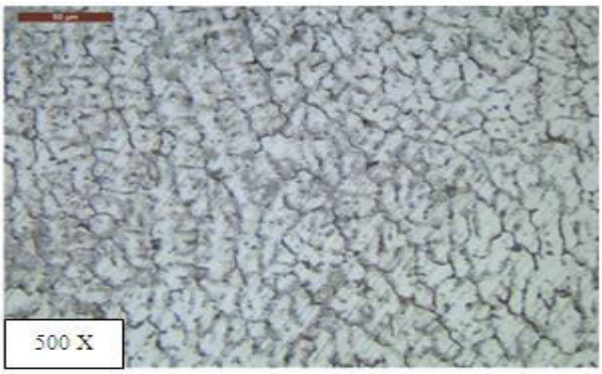

Figure-6(b). Fusion zone micrographs of heat applied sample of 175 A & 2 mm/s (500 X).

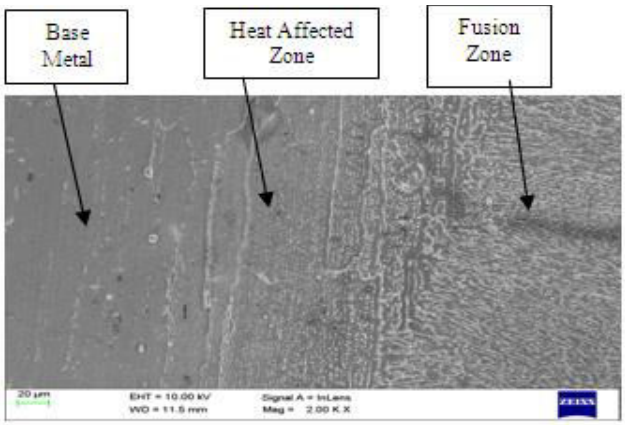

Figure-7. FE - SEM image of different zones of heat applied sample.

REINFORCEMENT OF TiC ONTO THE SURFACE OF AA 7075 ALLOY

TiC particles are reinforced onto the surface using GTA as a heat source. The average size of TiC particles was 106 µm. The reinforced surface samples were subjected to hardness measurements at fusion zone, heat affected zone and base metal. The hardness across the fusion zone increased from 124 HV to 160 HV on diffusing TiC particles into the aluminium matrix, this high hardness characteristic is due to the formation of high angle boundaries. They help avoid dislocations on the application of load [25].

Since the 7xxx series of aluminium alloys are age hardenable, post-weld heat treatment (PWHT) was carried out to improve the hardness of the weld zone. After the process of solution treatment, the hardness of the fusion zone dropped to 125 HV due to the dissolution of precipitates in the solid solution. The super saturated solid solution was formed because of rapid quenching. Finally, artificial aging was performed with various aging timing which results in hardness variation. The average hardness of the fusion zone for a distribution of time period ranging from 4-28 hours is shown in Figure-8. From the plot, it is observed that peak aging occurs at 20 hours with the hardness of 220 HV. The reinforced TiC particles along with the $MgZn_2$ precipitation help prevent dislocation from moving as a result, the hardness increases.

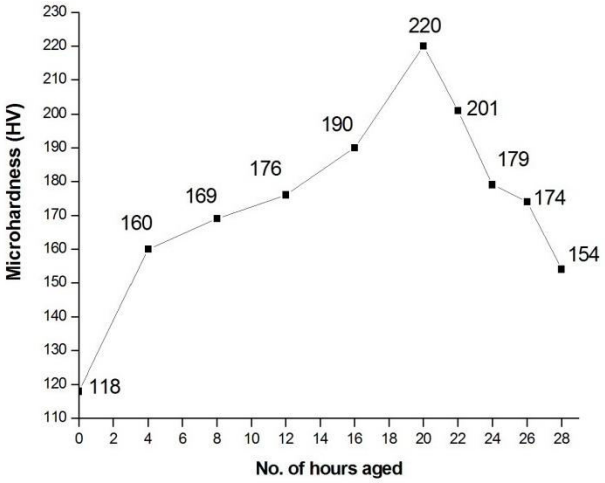

Figure-8. Average hardness of the fusion zone with the time period ranging from 4-28.

MICROSTRUCTURE AND XRD ANALYSIS OF TiC DIFFUSED AA 7075

The presence of TiC particles diffused within the aluminium matrix was indicated by FE-SEM as shown in Figure-9.

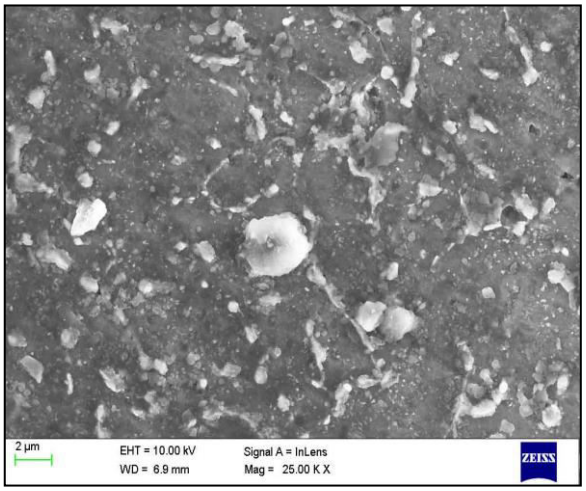

Figure-9. FE-SEM image of TiC particles in the AA 7075 surface.

The two main factors behind better distribution are the wettability of TiC with the molten aluminium matrix and the density difference between the aluminium matrix and the TiC particle. The density difference between TiC particles and AA 7075 aluminium alloy substrate is nearly 2g/cm^3. Due to such high-density difference, the TiC particles sink in the molten substrate on the application of heat [25]. The studies suggest that such suspension leads to a homogeneous distribution of particles within the aluminium matrix. Moreover, due to the good wettability of TiC particles with the aluminium, the free movement of TiC particles within the molten aluminium is avoided.

From the FE-SEM micrograph shown in Figure-9, it can be inferred that there is a clear interface between the TiC particle and the aluminium matrix, the high thermodynamic stability of TiC particles allows the surface to be clean and clear without the formation of undesirable compounds in the particle to matrix interface. The point EDX results show that Titanium and Carbon are present in significant amount in the melt and is represented in figure 10. In order to confirm the presence of Titanium carbide as a compound, XRD analysis was carried out and is shown inFigure-11. The pattern of compounds present in the diffused zone of AA 7075 is identified by XRD analysis. The compounds were confirmed based on reference code listed below:

- The reference code of 03-065-8803 corresponds to Titanium Carbide (TiC) presence.
- The reference code of 01-088-2321 refers to the presence of Titanium alone
- The reference code of 03-065-0120 indicates the presence of Magnesium Zinc ($MgZn_2$)on the diffused zone.
- The reference code of 01-079-5428 identifies the presence of Magnesium Silicide (Mg_2Si) precipitate.

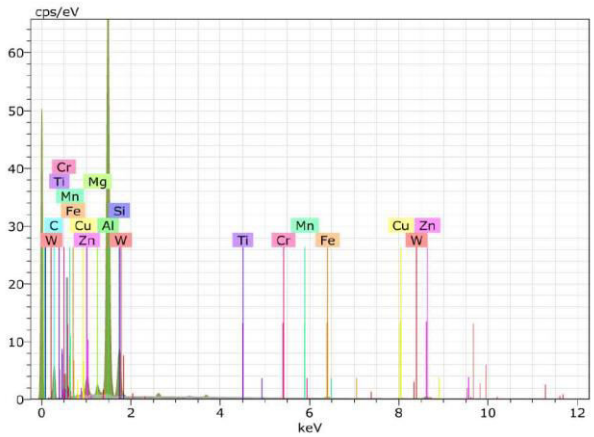

Figure-10. Point EDX scan of the surface composite.

On the whole, the diffraction peaks of the Titanium carbide, Magnesium Zinc ($MgZn_2$) and Magnesium Silicide (Mg_2Si) are confirmed. It also justifies the fact that Titanium carbide is thermally stable as there is no indication of other compounds present in the study.

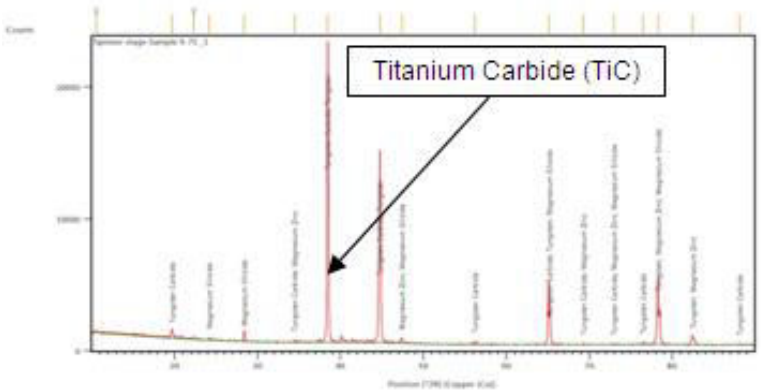

Figure-11. XRD analysis of the surface composite.

DRY SLIDING WEAR TEST RESULTS

Figure-12 reveals the effect of Load on the Wear rate of base metal, heat applied specimen and Tic diffused AA 7075 for the constant velocity of 1 m/s.

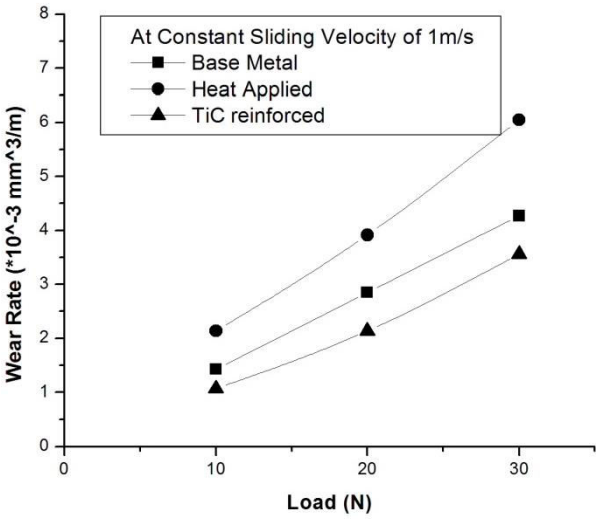

Figure-12. Load vs wear rate at sliding velocity of 1 m/s.

It can be observed that wear rate increases as the applied load increases. The occurrence of higher wear rate at higher load is similar to the findings of various researchers. There is an occurrence of debris on the matrix of aluminium alloy which ploughs the pin surfaces along the sliding direction, this result in severe plastic deformation of pin surfaces [26, 27, 28]. As a result, the wear rate is higher at higher loads in dry sliding environmental conditions. The highest wear rate was obtained for the load of 30 N and with the sliding velocity of 1m/s. The Base metal AA 7075 had a wear rate of 0.0043 mm^3/m, on the application of heat source the wear rate increased to 0.0060 mm^3/m and after the process of the surface refinement & heat treatment the wear rate reduced to 0.0036 mm^3/m.

Figure-13 reveals the effect of Sliding Velocity on the Wear rate of base metal, heat applied specimen and Tic reinforced AA 7075 respectively.

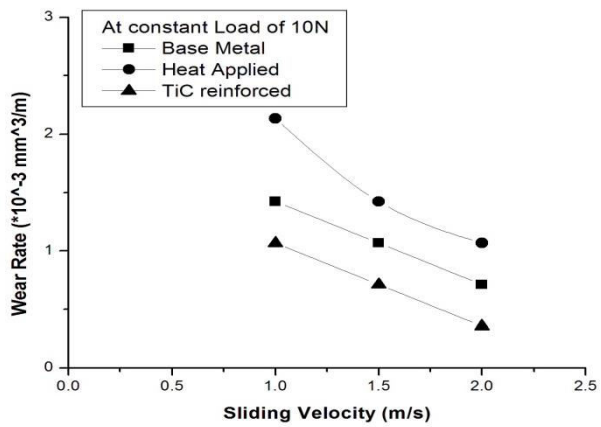

Figure-13. Sliding velocity vs wear rate at 10 N load.

At the operating conditions of 10N load and with the sliding velocity of 2 m/s, the wear rate was observed to be minimum. The wear rates of 0.0007 mm^3/m, 0.0011mm^3/m and 0.0004 mm^3/m were observed for the as received, heat applied and TiC reinforced sample respectively.

It is observed that wear rate decreases with the increase in sliding velocity from the Figure-13.It is reported that similar results of low wear rate at higher sliding velocity were obtained in C/ZrO2 composites [29]. When sliding under high-velocity conditions, the sliding surfaces experience a higher frictional force which in turn results in heat generation. At this high temperature, the soft aluminium matrix on the pin forms an oxide layer known as a mechanically mixed layer (MML) which causes smooth sliding between the pin and the disc surface, thereby resulting in a reduced wear rate [30].

On the basis of aliterature survey, it was found that the precipitate $MgZn_2$ dissolves on the application of heat and results in hardness reduction. The dissolution causes the aluminium matrix to become soft, as a result, there is higher plastic deformation causing higher wear rate for the heat applied samples. Whereas in the case of TiC reinforced samples, TiC particles increased the hardness of the surface. Moreover, the heat treatment was helpful in regaining the dissolved precipitates. This reduces the plastic deformation of the pin surface which in turn results in reduced wear rate.

Figure-14 indicates the variation of COF (μ) with a hardness of the alloy. For comparison basis, the load and sliding velocity are fixed at 30N and 2 m/s. It is observed that COF has a value of 0.3, with minor fluctuations. Hence, it can be concluded that COF is almost constant with respect to the hardness of the alloy [31].

Figure-15 shows the variation of wear rate for base, weld and surface refined substrates at 30N load and 1 m/s sliding velocity. On application of heat, the wear rate increased by 41% due to conditions described in the microstructure of heat applied specimen. Whereas, due to the process of TiC reinforcement, the wear rate of AA7075 reduced by 16% making it effective for tribological applications.

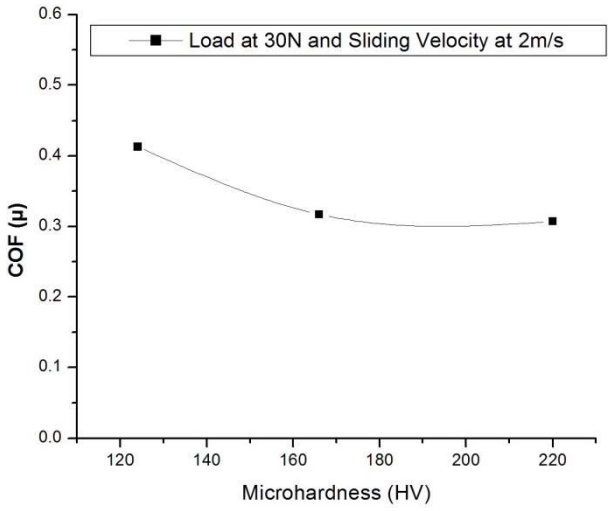

Figure-14. Hardness vs COF.

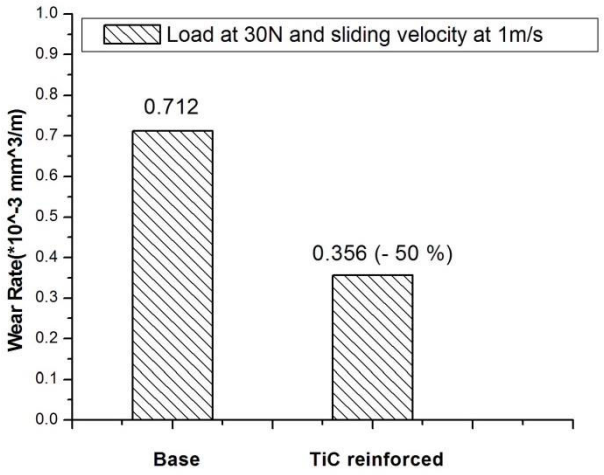

Figure-15. Variation of wear rate of TiC reinforced sample with respect to base sample.

4. CONCLUSIONS

AA 7075 aluminium alloy was reinforced with TiC using GTA as a heat source. The influence of TiC reinforcement on the hardness and wear resistance was studied. Based on the above analysis, following conclusions can be drawn:

- On application of heat, the precipitates dissolve and coarsening of constituent particles take place, which led to a reduction of hardness (26% for 150A, 6 mm/s) across the fusion zone.
- TiC was reinforced onto the surface of AA 7075 alloy using GTA as a heat source. Hardness across the fusion zone improved after depositing the TiC particles. Moreover, the hardness was further improved (33% with reference to base material) on PWHT owing to the distribution of strengthening precipitates ($MgZn_2$) in the matrix.
- Wear resistance of the TiC reinforced AA 7075 improved by 50 % with respect to base metal. variation of COF with respect to hardness was almost constant.

5. ACKNOWLEDGEMENTS

Special thanks must go to our professors Sanjivi Arul and R. Sellamuthu, for their technical guidance and discussions. In addition, the authors would like to thank M/s. PSGTECHS COE INDUTECH, Department of Textile Technology, Neelambur, Coimbatore, Tamilnadu, India for providing facility to carry out the material characterization work.

REFERENCES

[1] Wernick S., Pinner R. and Sheasby P.G. 1996. The Surface Treatment and Finishing of Aluminium and Its Alloys, 5th edition, pp. 2-4, ASM International, Materials Park, USA

[2] Kasthuri Raj, S.R., Ilangovan, S., Sanjivi Arul and Shanmugasundaram A. 2015. Effect of Variation in Al/Si Content on Mechanical Properties of Zn-Al-Si Alloys. International journal of applied engineering research. 10: 2723-2731.

[3] Suresh K.K., Ilangovan S., Sanjivi Arul and Shanmugasundaram A. 2015. Effect of Zn/Cu Content on Microstructure and Mechanical Properties of Al-Zn-Cu Cast Alloys. International journal of applied engineering research. 10: 9325-9333.

[4] Ramasundaram A., Ilangovan S., Sanjivi Arul and Shanmugasundaram A. 2015. Influence of Specimen Temperature on Wear Characteristics of Al-Zn-Mg Castings. International journal of applied engineering research. 10: 15417-15428.

[5] Devanathan R., Sanjivi Arul, Ilangovan S. and Shanmugasundaram A. 2015. Study on The Effect of Shallow Cryogenic Treatment on Hardness and Microstructure of GTAW welded AA6061 Specimens, International journal of applied engineering research. 10: 21091-21099.

[6] Rao R.N. and Das S. 2010. Effect of matrix alloy and influence of SiC particle on the sliding wear characteristics of aluminium alloy composites. Materials and Design. 31: 1200-1207.

[7] Srivatsan T. S., Sriram S. and Daniels C. 1995. The Influence of $A1_2O_3$ Particulate Reinforcement on Cyclic Stress Response and Fracture Behavior of 6061 Aluminum Alloy. Applied Composite Materials. 2: 175-198.

[8] Kaftelen H., Unlu N., Goller G., LutfiOvecoglu M. and Henein H. 2011. Comparative processing-structure-property studies of Al-Cu matrix composites reinforced with TiC particulates. Composites Part A. 42: 812-24.

[9] Straffelini G., Bonollo F. and Tiziani A. 1997. Influence of matrix hardness on the sliding behaviour of 20 vol% Al_2O_3-particulate reinforced 6061 Al metal matrix composite. Wear. 211:192-197.

[10] Michael Rajan H.B., Ramabalan S., Dinaharan I. and Vijay S.J. 2014. Effect ofTiB_2 content and temperature on sliding wear behaviour of AA7075/TiB2 in situ aluminium cast composites. Archives of Civil and Mechanical Engineering. 14: 72-79.

[11] Rajakumar S., Muralidharan C. and Balasubramanian V. 2011. Influence of friction stir welding process and tool parameters on strength properties of AA7075-T6 aluminium alloy joints. Materials and Design. 32: 535-549.

[12] Cavaliere, P., Cerri, E., Marzoli, L. and Dos Santos, J. 2004. Friction Stir Welding of Ceramic ParticleReinforced Aluminium Based Metal Matrix Composites. Applied Composite Materials. 11: 247-258.

[13] Paik J kee. 2009. Mechanical properties of friction stir welded aluminiumalloys 5083 and 5086. Inter J Nav Arch OcEngng. 1: 39-49.

[14] Wang X.H., Zhang M., Zou Z.D., Song S.L., Han F. and Qu S.Y. 2005. In situ production of Fe-TiC surface composite coatings by the tungsten-inert gas heat source. Surface and Coatings Technology. 200: 6117-6122.

[15] Hugh Pierson O. 1996. Handbook of Refractory Carbides and Nitrides. Noyes publication, New Jersey, USA.

[16] Polmear I.J. 1996. Light Alloys: Metallurgy of the Light Metals. 3rd edition, Wiley and Sons, New York, USA.

[17] Nie J., Muddle B. and Polmear I. 1996. The effect of precipitate shape and orientation on dispersion strengthening in high strength aluminium alloys. Materials Science forum. 217-222: 1257-1262.

[18] Poorhaydari K., Patchett B.M. and Ivey D.G. 2005. Estimation of Cooling Rate in the Welding of Plates with Intermediate Thickness. WeldingResearch Journal. pp. 149-155.

[19] Arul S. and Sellamuthu R. 2011. Application of a simplified simulation method to the determination of arc efficiency of gas tungsten arc welding (GTAW) and experimental validation. International Journal of Computational Material Science and Surface Engineering. 4: 265-280.

[20] Maloney S., Polmear, I. and Ringer S. 2000. Effects of Cu on precipitation in Al-Zn-Mg alloys. Materials Science Forum. 331-337:1055-1060.

[21] Ceschini L., Boromei I., Minak G., Morri A. and Tarterini F. 2007. Effects of friction stir welding on microstructure, tensile and fatigue properties of the AA7005 /10 vol. % Al_2O_3p composite. Composite Science and Technology. 67: 605-615.

[22] Vijaya Kumar P., Madhusudhan Reddy G. and Srinivasa Rao K. 2015. Microstructure, mechanical and corrosion behaviour of high strength AA7075 aluminium alloy friction stir welds - Effect of post weld heat treatment. Defence Technology. xx: 1-8.

[23] Wang X.H and Wang KS. 2006. Microstructure and properties of friction stir butt-welded AZ31 magnesium alloy. Material Science and Engineering A. 431:114-7.

[24] Sudhakar I., Madhusudhan Reddy G. and Srinivasa Rao K. 2016. Ballisticbehaviour of boron carbide reinforced AA7075 aluminium alloy using friction stir processing - An experimental study and analytical approach. Defence Technology. 12: 25-31.

[25] Han Y., Liu X. and Bian X. 2002. In situ TiB2 particulate reinforced near eutectic Al–Si alloy composites. Composites Part A. 33: 439-444.

[26] Arik H., OzcatalbasY. and Turker M. 2006. Dry sliding wearbehaviour of in situ Al-Al4C3 metal matrix composite produced by mechanical alloying technique. Materials and Design. 27: 799-804.

[27] Liu L., Li W., Tang Y., Shen B. and Hu W. 2009. Friction and wear properties of short carbon fiber reinforced aluminium matrix composites. Wear. 266: 733-738.

[28] Shorowordi K.M., Haseeb A.S.M.A. and Celis J.P. 2006. Tribo-surface characteristics of Al–B4C and Al-SiC composites worn under different contact pressures. Wear. 261: 634-641.

[29] Zhu H.G., Ai Y.L., Min J., Wu Q. and Wang H.Z. 2010. Dry sliding wear behaviour of Al-based composites fabricated by exothermic dispersion reaction in an Al–ZrO2-C system. Wear. 268: 1465-1471.

[30] Deuis R.L., Subramanian C. and Yellup J.M. 1997. Dry sliding wear of aluminium composites - a review. Composite Science and Technology. 57: 415-435.

[31] Singh J.B., Cai W. and Bellon P. 2007. Dry sliding of Cu-15 wt%Ni-8 wt%Sn bronze: Wear behaviour and microstructures. Wear. 263: 830-841.